Author Manuscript

Title: Discovery of Potential Mitochondrial Transcription Inhibitors as Anticancer Agents by Transcriptomic Profiling

Authors: Wenmin chen; Shuai Hu; Shuai Mao; Yibin Xu; Hui Guo; Haoxi Li; Michelle T. Paulsen; Xinde Chen; Mats Ljungman; Nouri Neamati, Ph.D.

Discovery of Potential Mitochondrial Transcription Inhibitors as Anticancer Agents by Transcriptomic Profiling

Wenmin Chen,[‡],[a] Shuai Hu,[‡, [a,b]] Shuai Mao,[a] Yibin Xu,[a] Hui Guo,[a] Haoxi Li,[a] Michelle T. Paulsen,[c], Xinde Chen,[a] Mats Ljungman,[c,d] Nouri Neamati[*,[a]]

a Departments of Medicinal Chemistry and Pharmaceutical Sciences, College of Pharmacy, Rogel Cancer center, University of Michigan, Ann Arbor, Michigan 48109, United States. E-mail:neamati@med.umich.edu

b Department of Computational Medicine and Bioinformatics, University of Michigan, Ann Arbor, Michigan 48109, United States

c Department of Radiation Oncology, Rogel Cancer Center and Center for RNA Biomedicine, University of Michigan, Ann Arbor, Michigan 48109, United States

d Department of Environmental Health Sciences, School of Public Health, University of Michigan, Ann Arbor, Michigan 48109, United States

‡ These authors contributed equally to this article

*Corresponding author

Abstract

Mitochondrial dysfunction is a hallmark of cancer cells and targeting cancer mitochondria has emerged as a promising anti-cancer therapy. Previously, we have repurposed nitrogen mustard chlorambucil by conjugating it with a mitochondrial targeting triphenylphosphonium (TPP) group to design compound Mito-Chlor that acts on mitochondria DNA (mtDNA). Herein, we show that the repurposed compound Mito-Chlor, but not chlorambucil, inhibits the nascent transcription of mtDNA using Bru-seq. Clustering analysis of transcriptomic profile of our Bru-seq database led to the identification of another mitochondrial transcription inhibitor SQD1, which inhibits the proliferation of MIA PaCa-2 cells at low micromolar range. However, Mito-Chlor reduces expression of mitochondrial proteins, interferes with mitochondria membrane potential, and impairs oxidative phosphorylation while SQD1 does not. Both compounds increased cellular and mitochondrial reactive oxygen species and stimulated similar signaling pathway. As mitochondrial transcription inhibitors and redox modulators, SQD1 and Mito-Chlor are promising for cancer treatment by manipulating mitochondrial function.

Introduction

Mitochondria are essential cellular organelles that serve as "powerhouses" to not only generate ATP through oxidative phosphorylation (OXPHOS), but also produce reactive oxygen species (ROS), control calcium signaling, and regulate cell cycle and differentiation.[1] The mitochondria of cancer cells undergo extensive bioenergetic and biosynthetic reprogramming to facilitate proliferation, invasion, and metastasis.[1] An increasing number of studies demonstrate that mitochondria has emerged as an important target for cancer treatment as the rapid proliferation of tumor cells is dependent on ample energy and biosynthesis product generated from the mitochondria [2]. Small molecules have been developed to act by targeting either mitochondrial DNA (mtDNA) or mitochondrial proteins.

mtDNA is a compact circular genome without introns and is transcribed as part of single transcripts generated from either the heavy or light strand of the genome, encoding 13 proteins that constitute essential subunits of mitochondrial respiratory chain complexes (I-IV) [3]. It has been shown that tumorigenicity is reduced following the elimination of mtDNA by ethidium bromide [4]. A number of anti-cancer agents cause decreases in mtDNA levels, such as the nucleoside derivatives zidovudine and zalcitabine, and this correlates with their cytotoxicity [5]. Anti-cancer drug ditercalinium causes mtDNA depletion and disrupts its replication via an interaction with the mitochondrial DNA polymerase γ and the mitochondria-specific helicase Twinkle [6].

Importantly, cancer cells have higher intrinsic mitochondrial membrane potential ($\Delta\psi$mt) than normal cells. An effective approach to generate small molecules targeting cancer cell mitochondria is to conjugate a lipophilic cation, such as a triphenylphosphonium (TPP$^+$) moiety, to the drug of interest.[7] Previously, we developed a TPP-derivative of the nitrogen mustard chlorambucil (**Fig. 1A**), a DNA alkylating drug approved by the FDA for the treatment of chronic

lymphocytic leukemia and lymphomas.[8] This TPP-conjugated chlorambucil, named Mito-Chlor, selectively localizes to mitochondria, where it acts on mtDNA and causes cell cycle arrest and cell death.[8]

This study expanded current understanding of Mito-Chlor and identified it as a potent mitochondrial transcription inhibitor. Comparing Bru-seq data from other novel small molecules led to the identification of another mitochondrial transcription inhibitor SQD1 (**Fig. 1A**), which exhibits anti-cancer activities against a panel of cell lines. SQD1 shares a similar transcriptomic profile with Mito-Chlor, and we thereby characterized it in parallel with Mito-Chlor to further elucidate their mechanisms of action. This study demonstrates that blockade of mitochondrial transcription might be a novel strategy for treatment of cancer.

Result and discussion

Chemistry

The synthesis of **SQD1** is depicted in Scheme 1. Nitroquinolone **4** was synthesized as previously described.[9] The arylaminomethylene meldrum's acid **2** was prepared by a modified Polansky's method: the solution of meldrum's acid was heated in methylorthoformate under reflux for 2 h, followed by the addition of arylamine **1**. The mixture was heated under reflux for an additional 5 h. Subsequent regioselective nitration of compound **2** with nitric acid supported on silica gel in dichloromethane afforded **3**. Compound **3** was cyclized to the corresponding nitroquinolone **4** in diphenyl ether at 250 °C for 15 min. Treatment of quinolone **4** with $POBr_3$ in DMF gave the 4-bromoquinoline **5**. Intermediate **5** underwent the Heck coupling reaction with the respective substituted (*E*)-styrylboronic acid in dioxane using $Pd(PPh_3)_4$ as a catalyst to produce **6**. Subsequent reduction of the nitro group of **6** with activated iron provided daniline product **7**, which

was then reacted with appropriate butyryl chloride in the presence of trimethylamine to afford **8**. The final oxidation of **8** with ceric ammonium nitrate in acetonitrile and H_2O gave the desired compound **9** (**SQD1**).
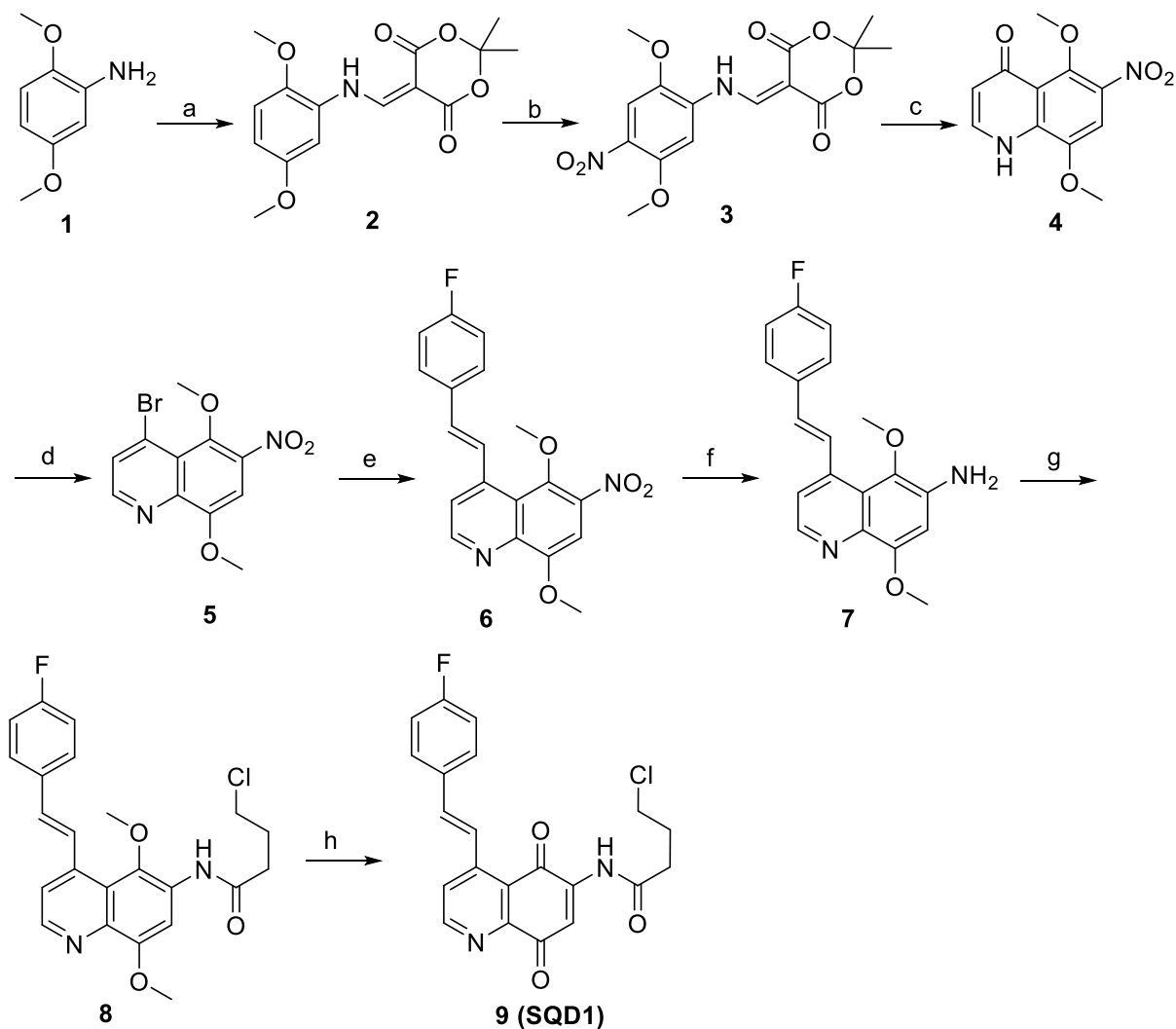
Scheme 1. The synthesis of **SQD1**. Reagents and conditions: (a) Meldrum's acid, methylorthoformate, reflux, 7 h; (b) HNO_3/SiO_2, CH_2Cl_2, RT; (c) PhOPh, 250 °C, 15 min; (d) $POBr_3$, DMF, 0 °C – RT; (e) $Pd(PPh_3)_4$, K_2CO_3, dioxane, H_2O, reflux, 6 h; (f) Fe, AcOH, MeOH, H_2O, reflux, 30 min; (g) $Cl(CH_2)_3COCl$, TEA, THF, 0 °C –RT, overnight; (h) $(NH_4)_2Ce(NO_3)_6$, CH_3CN, H_2O, 0 °C – rt, 2 h.

Mito-Chlor and SQD1 inhibit the transcription of the mitochondrial genome.

Mito-Chlor was shown to accumulate in mitochondria and act on mtDNA, setting it apart from its parent compound chlorambucil.[8] To expend our knowledge of this mitochondria targeting agents, we used Bru-seq technique to interpret its influence on the mitochondria transcription.[10]

The circular mitochondrial genome contains a guanine-rich heavy (H-strand) and a guanine-poor light strand (L-strand).[11] H-strand and L-strand are transcribed independently, controlled by the light-strand promoter (LSP), the heavy-strand promoter 1 (HSP1) and the heavy-strand promoter 2 (HSP2), which are located nearby in the displacement loop (D-loop), the main non-coding region of the mtDNA.[11] The H-strand encodes 12 mitochondrial proteins, such as ATP6 and CYB, while the L-strand only encodes ND6 (**Fig. 1B**).[12] These proteins constitute essential subunits of the four mitochondrial respiratory chain complexes. In the Bru-seq trace diagrams of mitochondrial transcripts, remarkably, after a 4-hour treatment in MIA PaCa-2 cells, Mito-Chlor inhibited transcription from the HSP1 and HSP2, while having no detectable effect on transcription from the LSP. In contrast, chlorambucil showed no inhibitory effect on either of the two strands (Fig. 1C). This result confirms the successful delivery of Mito-Chlor into mitochondria. Mito-Chlor was found to achieve 80-fold enhancement of anticancer activity against a panel of breast and pancreatic cancer cell lines. Importantly, Mito-Chlor delayed tumor progression in a mouse xenograft model of human pancreatic cancer. [8]

As targeting mtDNA has emerged as a potential anticancer therapy, we performed a robust cluster analysis using a collection of over 100 in-house compounds analyzed by Bru-seq (Supplementary Figure 1) to identify other small molecules with similar mechanism to Mito-Chlor. This analysis led to the identification of a novel compound SQD1, featuring a unique

styrylquinoline-5, 8-dione core (**Fig. 1A**). SQD1 shares a similar genome-wide transcription profile with Mito-Chlor, and interestingly, it is also found to block the mitochondria transcription from LSP, HSP1 and HSP2 (**Fig. 1C**). Additionally, H_2O_2 inhibited mitochondrial transcription from the HSP1 and HSP2 in a dose-dependent manner (**Fig. 1C**), indicating that ROS could cause mitochondrial transcription inhibition.
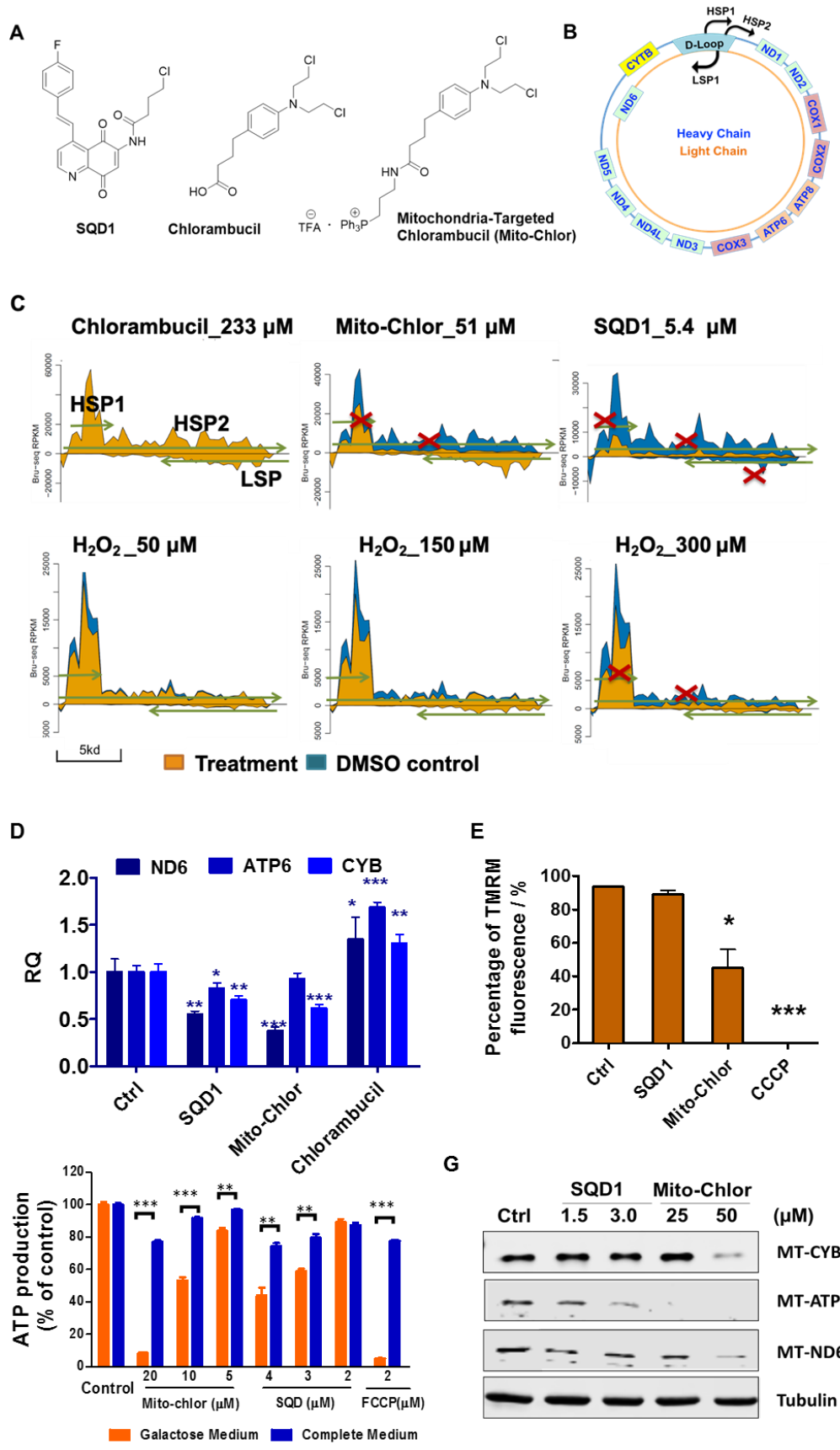
We next conducted real-time PCR (RT-PCR) to detect the mRNA levels of mitochondrial genes located on both strands of the circular mtDNA (**Fig. 1D**). MT-ND6 (mitochondrially encoded NADH: ubiquinone oxidoreductase core subunit 6) is the only protein-coding gene on the L-strand, and MT-ATP6 (mitochondrially encoded ATP synthase membrane subunit 6) and MT-CYB (mitochondrially encoded cytochrome B) are two protein-coding genes on the H-strand. Similar to the Bru-seq results, SQD1 significantly decreased the transcription of ATP6, CYB and ND6 genes, confirming that SQD1 inhibited mitochondrial transcription from all promoters (**Fig 1D**). Mito-Chlor reduced the steady-state level of ND6 transcripts controlled by LSP, which was not observed in the nascent RNA Bru-seq. Furthermore, Mito-Chlor decreased CYB transcription, not ATP6 transcription, although both genes are encoded by the H-strand (**Fig. 1D**). In contrast to Mito-Chlor, chlorambucil did not inhibit the steady-state RNA levels of any of these three genes (**Fig. 1D**). It is interesting to note the different results obtained with Bru-seq and RT-PCR of Mito-Chlor. A potential explanation for this is that RT-PCR quantifies the steady-state levels of total RNAs while Bru-seq only measures the newly synthesized RNA.

The mitochondrial membrane potential ($\Delta\Psi$m, MMP), generated by proton pumps, is critical for the physiological function of mitochondria. We next investigated whether these agents would affect MMP using tetramethylrhodamine methyl ester (TMRM), a cell-permeable dye that accumulates in active mitochondria with intact membrane potentials. After a 4-hour treatment,

Mito-Chlor displayed significant decrease in the TMRM fluorescence level while SQD1 did not (**Fig. 1E**), suggesting that Mito-Chor also interfered with mitochondrial physiological function while SQD1 did not.

In order to assess the effects of SQD1 and Mito-Chlor on mitochondrial OXPHOS, we measured the ATP production in compound-treated MIA PaCa-2 cells in glucose and galactose medium (**Fig. 1F**). In the glucose medium, mammalian cells generate ATP from both aerobic glycolysis in cytoplasm and mitochondrial OXPHOS. Galactose medium where galactose is the sole sugar source for mammalian cells will force them to rely on mitochondrial OXPHOS, instead of glycolysis, to produce ATP.[13] FCCP (carbonyl cyanide-4-(trifluoromethoxy)phenylhydrazone) the uncoupler of mitochondrial OXPHOS was used as a positive control.[14] After 24-hour treatment, 2 μM FCCP, the uncoupler of mitochondrial OXPHOS showed a significant decrease in ATP production in galactose medium as compared to glucose medium, so did Mito-Chlor at 20 μM , while only marginal difference was observed with SQD1 at all three test concentrations (**Fig. 1F**). This result suggests that the Mito-Chlor impaired ATP production by the mitochondrial OXPHOS while SQD1 did not.

Furthermore, we performed immunoblot on three mitochondrial proteins to assess their protein expression (**Fig. 1G**). Mito-Chlor (50 μM) remarkably decreased in protein levels of CYB, ATP6 and ND6 while SQD1 showed no reduction of these proteins. Taken together, although both SQD1 and Mito-Chlor inhibit the nascent transcripts of mtDNA as indicated by Bru-seq, Mito-Chlor finally decreases mitochondrial protein expression, impairs mitochondrial physiological function and inhibits mitochondrial OXPHOS. However, the effects of SQD1 is limited on mitochondrial transcription level. Therefore, Mito-Chlor has a more solid profile on regulating mitochondrial function, in terms of transcripts, proteins, and function.

Author Manuscript

A

SQD1 Chlorambucil TFA · Ph₃P Mitochondria-Targeted Chlorambucil (Mito-Chlor)

B

C

Chlorambucil_233 µM   Mito-Chlor_51 µM   SQD1_5.4 µM

HSP1   HSP2   LSP

H₂O₂_50 µM   H₂O₂_150 µM   H₂O₂_300 µM

5kd   ■ Treatment   ■ DMSO control

D

E

F

Z

G

SQD1   Mito-Chlor

Ctrl   1.5   3.0   25   50   (µM)

MT-CYB
MT-ATP6
MT-ND6
Tubulin

Figure 1. The effects of SQD1 and Mito-Chlor on mitochondrial transcription, mitochondrial proteins, and ATP production. **(A),** Structures of SQD1, chlorambucil, and Mito-Chlor. **(B),** Transcription from the mitochondrial genome occurs on the L-strand (orange) and the H-Strand (blue) controlled by three promoters, HPS1, HSP2, and LSP1. **(C),** Bru-seq trace diagrams of the transcription of the mitochondrial genome after treatment with chlorambucil, Mito-Chlor, SQD1, and H_2O_2 in MIA PaCa-2 cells. Chlorambucil showed no effects on mitochondrial transcription, while Mito-Chlor blocked the transcription from the H-strand promoters. SQD1 treatment inhibited transcription from all three promoters. H_2O_2 treatment displayed modest inhibition of transcription from the H-strand promoters. **(D),** SQD1 and Mito-Chlor reduce mitochondrial RNA levels of CYB, ATP6, and ND6 genes as represented by relative quantification (RQ) values determined from RT-PCR. Treatment conditions are the same as the Bru-seq experiments. * denotes $p < 0.05$, ** $p < 0.005$, and *** $p < 0.0005$. **(E),** TMRM measurement of MMP in MIA PaCa-2 cells treated by SQD1 and Mito-Chlor at 4 h. CCCP was used as a positive control. Treatment conditions are the same as the Bru-seq experiments. **(F),** The measurement of ATP production in MIA PaCa-2 cells cultured in in glucose and galactose medium after treatment with SQD1, Mito-Chlor, and FCC for 24 h. (**G**), Immunoblot of MT-CYB, MT-ATP6, and MT-ND6 at 24 h treatment.

Mito-Chlor and SQD1 induce similar transcription profiles.

Besides the effects on mitochondrial transcription, we further analyzed genome-wide transcriptomic profile of SQD1 and Mito-Chlor to understand its working mechanism in the cells. SQD1- and Mito-Chlor-treated samples have in total 12,336 common expressed genes with a good Pearson correlation (r) of 0.52 ($p < 2.2e–16$) (**Fig. 2A**). The common upregulated genes ($\log_2FC > 1$) have an r value of 0.45 ($p < 2.2e–16$), and their common downregulated genes ($\log_2FC < –1$)

have an r value of 0.34 ($p < 2.2e–16$) (**Fig. 2B, 2C**). Remarkably, 19 of top 25 upregulated and 19 of top 25 downregulated protein-coding genes from SQD1 treatment were also altered in the Mito-Chlor-treated sample in the same direction (Highlighted in Supplementary Table 1).

Examining the common upregulated genes (Supplementary Table 1) induced by SQD1 and Mito-Chlor revealed some clues to their common mechanism of action. *HMOX1*, with the highest fold change in both SQD1 (FC=315.4) and Mito-Chlor (FC=206.6) treated samples, encodes heme oxygenase 1 (HO-1), an important protein for cellular defense against oxidative injury.[15] The transcription of other oxidative stress defense genes OSGIN1 and SESN2 are also induced. Transcripts of coding genes related to unfolded protein response (UPR) (*CHAC1*, *ASNS* and *DNAJB4*) and synthesis or transportation of cysteine (*SLC7A11* and *CTH*) are also up regulated [16]. The activation of the *UPR* on exposure to oxidative stress is an adaptive mechanism to preserve cell function and survival.[16b] Cysteine is an essential substrate for the synthesis of the primary cellular antioxidant glutathione (GSH) [17], which maintains the thiol status of critical proteins and defends against ROS via its reducing capacity. [18] Altogether, these findings indicate the treatment of SQD1 and Mito-Chlor have rendered extensive oxidative insults in MIA PaCa-2 cells. The nascent transcriptional expression of several transcription factors (*CEBPB*, *DDIT3*, and *LMO4*) and autophagosomal-related gene (*MAP1LC3B*, and *GABARAPL1*) [19] were also observed, indicating the enhancement of transactivation and autophagy.

Gene set enrichment analysis (GSEA) is a computational method that identifies classes of genes that are over-represented in a large set of genes.[20] According to the GSEA results, Mito-Chlor shares much fewer common genes and gene sets with its parent compound chlorambucil than with SQD1 (Supplementary Figure 2, Supplementary Tables 4, 5, 6), confirming the repurposing of Mito-Chlor. [8] Specifically, 7 out of the top 20 upregulated gene sets and 10 out of

the top 20 downregulated gene sets are in common between SQD1 and Mito-Chlor. The gene sets related to hypoxic response and redox signaling are induced while the ones related to cell growth and differentiation are suppressed (Supplementary Table 2,3,4; **Fig. 2D, 2E**). The top one common up-regulated gene set is PODAR_RESPONSE_TO_ADAPHOSTIN_UP. Adaphostin is known to kill cancer cells through a mechanism that involves up-regulation of ROS. Moreover, adaphostin is concentrated several thousand folds in mitochondria, where it inhibits complex III of the respiratory chain and leads to mitochondrial ROS generation. [21] The GESA results strongly suggest the vital roles of oxidative stress and mitochondria function in the pathway triggered by Mito-Chlor and SQD1.
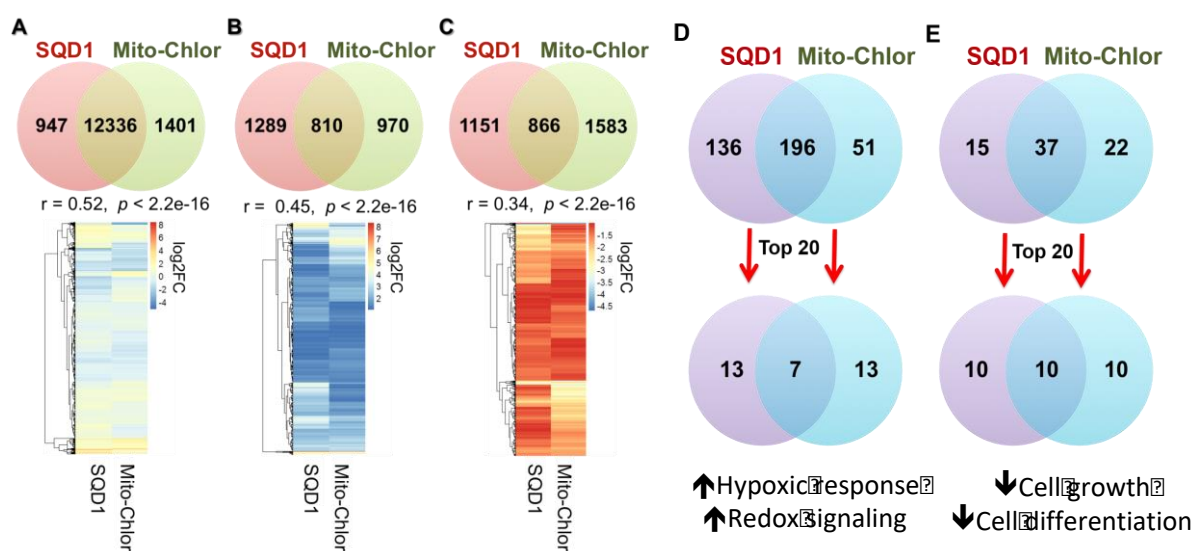

Figure 2. SQD1 and Mito-Chlor share similar transcriptomic profiles and enriched gene sets. The comparisons between SQD1 and Mito-Chlor are displayed in heatmaps. (**A**)**,** Total common genes. (**B**)**,** Common upregulated genes. (**C**)**,** Common downregulated genes. r is Pearson correlation. SQD1 and Mito-Chlor also share common (**D**)**,** upregulated and (**E**)**,** downregulated enriched gene sets with FDR < 0.001. Top 20 enriched gene sets ranked by FDR values were also compared between the two samples.

Evaluation of the cytotoxicity and ROS induction capability of SQD1 and Mito-Chlor.

We used CM-H2DCFDA dye, a general oxidative stress indicator, to measure ROS induced by SQD1 and Mito-Chlor.[22] Relative fluorescence unit (RFU) represents the relative level of cellular ROS. SQD1 induced a moderate increase in the fluorescence while Mito-Chlor caused a significant increase in a time-dependent manner (**Fig. 3B**). Moreover, the elevated fluorescence signal could be attenuated by ROS scavenger and antioxidant NAC and Vit-E (**Fig. 3C**). Dihydroethidium (DHE) was used as an independent redox probe for the detection of superoxide and hydrogen peroxide.[23] The histogram shows a right shift of the DHE fluorescence in SQD1- and Mito-Chlor-treated samples as compared with the control, suggesting increased oxidative stress (**Fig. 3D**). Given the mitochondrial transcription inhibition effect of SQD1 and Mito-Chlor, we next assessed mitochondrial superoxide level using the MitoSOX Red dye.[24] Mitochondrial complex III inhibitor, antimycin A, a well-established stimulus of mitochondrial superoxide and ROS production was used as a positive control. SQD1, Mito-Chlor and antimycin A treatment increased fluorescence signal due to the induction of mitochondrial superoxide (**Fig. 3E**). In contrast, chlorambucil and TPP control groups did not alter the mitochondrial superoxide level (Supplementary Figure 3). Taken together, these results confirm that SQD1 and Mito-Chlor could increase cellular ROS especially mitochondria superoxide in MIA PaCa-2 cells.
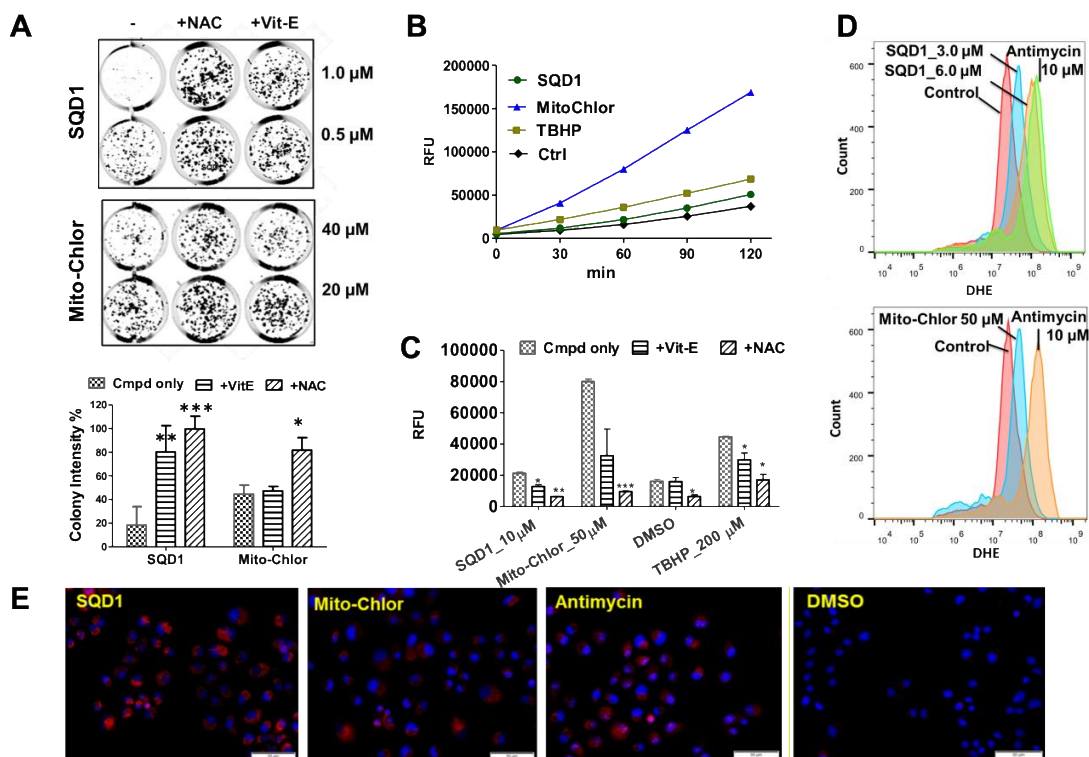
Figure 3. SQD1 and Mito-Chlor inhibit cell growth and increase ROS levels in MIA PaCa-2 cells. **(A),** NAC (2.0 mM) or Vit-E (0.5 mM) protect cytotoxicity of SQD1 and Mito-Chlor. **(B),** Relative fluorescence unit (RFU) was measured at indicated time using CM-H$_2$DCFDA dye. *Tert*-Butyl hydroperoxide (TBHP) was used as a positive control. **(C),** The RFU of compound-treated MIA PaCa-2 cells in the presence or absence of Vit-E (0.5 mM) or NAC (3 mM) after 1-hour treatment. * denotes $p < 0.05$, ** denotes $p < 0.005$. **(D),** Detection of superoxide and hydrogen peroxide in MIA PaCa-2 cells treated with SQD1 (5.4 μM), Mito-Chlor (51 μM), antimycin A (15 μM) or DMSO using DHE dye. **(E),** Detection of mitochondrial superoxide using MitoSOX Red superoxide indicator (2 μM) with fluorescence microscope. Objective: 20x.

Antiproliferative activity of SQD1 was evaluated in MIA PaCa-2 cells in parallel with Mito-Chlor (Table 1). SQD1 inhibited the proliferation of MIA PaCa-2 with an IC$_{50}$ value at low micromolar range, 40-fold higher than Mito-Chlor. Additionally, SQD1 inhibited the proliferation

of a panel of cancer cells at low micromolar range (Supplementary Table 6). Both SQD1 and Mito-Chlor induced PARP-1-mediated cell death pathway in MIA PaCa-2 cells (Supplementary Figure 4).

The combination of antioxidant vitamin E (Vit-E) slightly reduced the cytotoxicity of SQD1, again, suggesting that elevated oxidative stress within cells may contribute to their cytotoxicity. The combination with antioxidant and nucleophilic scavenger N-acetyl cysteine (NAC) significantly decreased the cytotoxicity of SQD1, implying that intracellular thiol-containing molecules may contribute to the detoxification of SQD1 (**Table 1, Fig. 1A**). The rescue effect of NAC and Vit-E was also observed for Mito-Chlor, indicating that the cytotoxicity of Mito-Chlor is linked to ROS (**Table 1, Fig. 1A**). Taken together, these results show that both SQD1 and Mito-Chlor elevated cellular and mitochondria superoxide, which contributes to their cytotoxicity.

Table 1. Cytotoxicity IC_{50} (μM)^a of SQD1 and Mito-Chlor in MIA PaCa-2 cells.

ID	Compound only	+2 mM NAC	+0.5 mM Vit-E
SQD1	1.3±0.2	9.8±3.8	2.1±0.6
Mito-Chlor	42.0±2.0	>50	>50

^{a}IC_{50} data are shown as mean ± standard deviation from three independent experiments. ^{b}Not tested.

SQD1 and Mito-Chlor induced similar protein expression patterns.

Immunoblot analysis of the top upregulated genes' coding proteins revealed that SQD1 treatment caused a robust increase in the expression of 8 proteins (**Fig. 4**). These proteins are mostly involved in oxidative stress (SESN2, HMOX1), transactivation (FOSB, C-JUN), metabolism regulation (HK2, PFKFB4), and induction of autophagy (MAPLC-3α/β, GABARAPL). The protein FOS dimerizes with JUN to form the transcription factor complex AP-

1, [25] The substantial upregulation of the components of transcription activator AP-1, JUN and FOS (**Fig. 4**) are likely to be responsible for the strong trend of transcription activation induced by the two compounds. As previously discussed, the most upregulated gene, HMOX1, its protein expression level increased during oxidative injury.[15, 26] Protein sestrin coded by SESN2 is another antioxidant induced under oxidative and genotoxic stress to protect cells against ROS was also significantly upregulated.[27] The mitochondrial genome is especially vulnerable to oxidative damage since it does not contain protective histones.[28] Oxidatively damaged mitochondria can be eliminated through autophagy to prevent excessive ROS production.[29] The significant increase in GABARAPL and MAPLC-3α/β levels may indicate the induction of autophagy. SQD1 also upregulated protein expression of HK2 and PFKFB4, suggesting enhanced glycolysis (**Fig. 4**).

H_2O_2 triggered similar changes in protein levels of FOSB, c-JUN, HMOX1, SESN2, MAPLC-3α/β, and GABARAPL which are observed post-treatment of SQD1 (**Fig. 4**). The antioxidant NAC attenuated the protein changes caused by SQD1 and H_2O_2, supporting the hypothesis that the induced cellular ROS had profound influences on the downstream signaling of SQD1 (**Fig. 4**). Mito-Chlor also dose-dependently induced the expression levels of HMOX1, SESN2, FOSB, MAPLC3α/β, and c-JUN proteins, like SQD1 (**Fig. 4A, 4B**). However, the protein levels of glycolytic enzyme HK2, PFKFB4, and autophagy-related protein GABARAPL were not altered by Mito-Chlor treatment (**Fig. 4A, 4B**). The addition of NAC protected the upregulation of transcription activator AP-1 and HMOX1 induced by Mito-Chlor but had negligible influence on the expression levels of SESN2 and MAPLC3α/β (**Fig. 4A**).
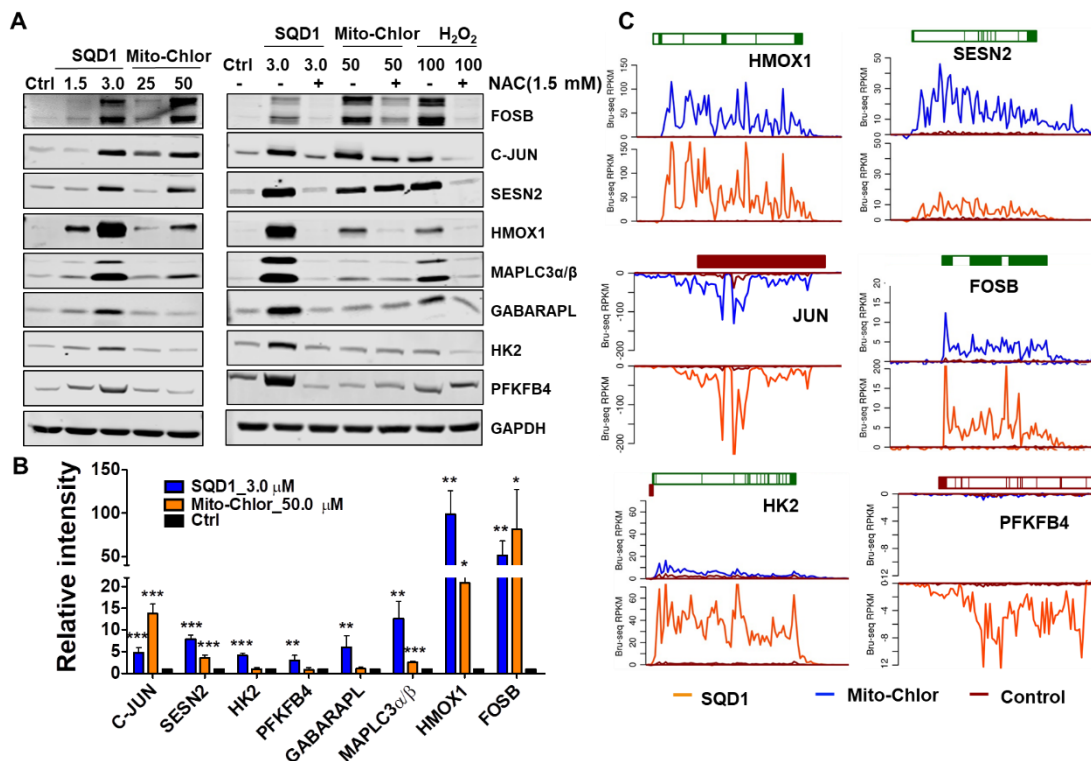
Figure 4. SQD1, Mito-Chlor, and H_2O_2 induced similar changes in protein expression in MIA PaCa-2 cells. **(A),** 24 h treatment of SQD1 upregulated the expression levels of FOSB, c-JUN, HMOX1, HK2, PFKFB4, MAPLC-3α/β, and GABARAPL in a dose-dependent manner. Mito-Chlor treatment induced similar protein expression changes with the exception of GABARAPL, HK2, and PFKFB4. SQD1-, Mito-Chlor- and H_2O_2-induced changes in select protein levels were rescued by the addition of 1.5 mM NAC. **(B),** Protein levels induced by SQD1 and Mito-Chlor were quantified by ImageJ and normalized to respective loading controls. The data are presented as mean ± standard deviation of at least three independent experiments. * denotes $p < 0.05$, ** denotes $p < 0.005$, and *** denotes $p < 0.0005$. **(C),** Transcription trace diagrams of the representative genes after SQD1 or Mito-Chlor treatment. The positive y-axis represents the plus-strand signal of transcription moving from left to right, and the negative y-axis represents the minus-strand signal of transcription moving from right to left.

Conclusion

Cancer cells have higher intrinsic mitochondrial membrane potential than normal cells, which makes directing the bioactive agents through conjugating with lipophilic cations to be a feasible strategy for targeting cancer cells. TPP-conjugated nitrogen mustard Mito-Chlor has been designed to enter mitochondria where it alkylates mtDNA.[8] Herein, we expanded current understanding of Mito-Chlor, which it also inhibits the transcription of mtDNA and decreases the level of mitochondrial proteins, while its parent compound, chlorambucil, does not. A search of in-house small molecules that share similar nascent transcriptomic profile with Mito-Chlor led to the discovery of SQD1, which also blocks the transcription of mtDNA. SQD1 and Mito-Chlor are promising tool molecules for regulating mtDNA transcription, while the influence of Mito-Chlor on mitochondria is more profound than SQD1.

In addition, we also elucidated that SQD1 and Mito-Chlor induce cellular ROS, especially mitochondria ROS (**Fig. 5**). Their redox-modulating capability could partially contribute to the mitochondrial transcription inhibition because H_2O_2 only is able to cause mitochondrial transcription inhibition (**Fig. 1**). However, their transcription inhibition pattern and the pathways to ROS induction could be different. The mitochondrial superoxide increased by Mito-Chlor is likely to be a downstream effect of its mtDNA alkylating and damaging effect. SQD1, as a quinone redox recycler, has the capacity to produce radical species when it is reduced to semiquinone by cytochrome P450 oxidoreductase. It may also react with cysteines of some proteins, deplete GSH or alkylate DNA, resulting in cellular oxidative stress (**Fig. 5**). mtDNA is not protected by histones and mitochondria has limited DNA repair capacity,[30] which make it very susceptible to oxidative insults caused by ROS. mtDNA damage is involved in transcription arrest by transcriptional mutagenesis or premature transcript termination [31]. mtDNA damage eventually

alters mitochondrial gene expression, causes impairment of the respiratory complexes and a concomitant increase in mitochondrial ROS, leading to a vicious feed-forward cycle of additional mtDNA damage and ROS production.[28]

This study demonstrates that Bru-seq is a useful approach for elucidating the small molecules' mechanism of action of and clustering analysis of transcriptomic profile is very useful for identifying compounds with similar mechanism of action. Overall, this work not only disclosed two mitochondrial transcription inhibitors with efficient anticancer activity but also proposed an efficient drug discovery strategy based on transcriptomic profiling.

Experimental Section

General. All commercial chemicals and solvents used for synthesis were reagent grade and were used without further purification unless otherwise specified. Analytical thin layer chromatography was performed on EMD Millipore TLC Silica Gel 60 F254 to follow the course of reactions. Column chromatography was performed using SiliaFlash P60 silica gel (40–63μm, 60Å). Proton nuclear magnetic resonance (^{1}H NMR) spectroscopy was performed using a Bruker Utrashield 300 or a Bruker Ascend 400 NMR spectrometer. Chemical shifts (δ) are reported in parts per million (ppm) relative to an internal standard. The following abbreviations are used to describe peak splitting patterns: s (singlet), d (doublet), t (triplet), q (quartet), m (multiplet), dd (doublet of doublets), td (triplet of doublets). Coupling constants (J) are expressed in hertz unit (Hz). The purity was checked by Shimadzu 2030C 3D liquid chromatography module using Shimadzu HPLC Test Kit C18 reverse phase column (3 μm, 4.6 x 50mm) with acetonitrile and water as the gradient. All the final compounds were confirmed to have purity > 95%. Mass spectrum analysis was performed on a Shimadzu 2020 liquid chromatography mass spectrometer.

Chlorambucil was purchased from Oakwood Products, Inc., and Mito-Chlor was synthesized as described (12).

Synthesis of 4-bromo-5,8-dimethoxy-6-nitroquinoline (5). A suspension of nitroquiolone **4** (84 mg, 0.034 mmol) in DMF was added $POBr_3$ dropwise at 0°C. The suspension became clear and then cloudy during this process. After 1h, the reaction mixture was diluted with 28% ammonia aqueous solution and extracted with ethyl acetate. The combined extracts of organic solvent were washed with brine, dried over anhydrous Na_2SO_4 and evaporated under vacuum. The residue was purified on flash column chromatography with ethyl acetate and hexane as elution to give compound **5** as a colorless oil (8.5 mg, yield 80%). ^{1}H NMR (400 MHz, $CDCl_3$) δ 8.79 – 8.68 (m, 1H), 7.90 (d, J = 4.6 Hz, 1H), 7.40 (d, J = 2.4 Hz, 1H), 7.26 (s, 1H), 4.13 (s, 3H), 3.98 (s, 3H). LC-MS: m/z= 313.05, 315.02 $[M+H]^+$

Synthesis of (E)-4-(4-fluorostyryl)-5,8-dimethoxy-6-nitroquinoline (6). Compound **5** (10 mg, 0.068 mmol), (*E*)-(4-fluorostyryl)boronic acid (11 mg, 0.068 mmol) and K_2CO_3 (11 mg, 0.081 mmol) were introduced in a 25 mL round-bottom flask degassed with nitrogen gas. The mixture of 1,4-dioxane and water (5 mL, 4:1) were added and then stirred for 5 min, followed by the addition of $Pd(PPh_3)_4$ (4 mg, 0.003 mmol). The mixture was refluxed for 6 h under a nitrogen atmosphere. The organic phase was evaporated and residue was purified by column chromatography to give **6** (8 mg, yield 71%). ^{1}H NMR (400 MHz, $CDCl_3$) δ 8.98 (d, J = 4.6 Hz, 1H), 8.15 (d, J = 16.1 Hz, 1H), 7.62 (d, J = 4.3 Hz, 1H), 7.60 – 7.55 (m, 2H), 7.40 (s, 1H), 7.14 – 7.06 (m, 3H), 4.13 (s, 3H), 3.79 (s, 3H). LC-MS: m/z= 355.15 $[M+H]^+$

Synthesis of (E)-4-chloro-N-(4-(4-fluorostyryl)-5,8-dimethoxyquinolin-6-yl)butanamide (8) To a refluxing solution of methanol (8 mL), glacial acetic acid (1 mL) and water (1 mL) were added compound **6** (200 mg, 0.56 mmol) and iron powder (158 mg, 2.82 mmol). The mixture was

refluxed for another 30 min with vigorous stirring. The reaction solution was filtered through celite. The organic phase of the filtrate was removed under vacuo and the residue was added saturated aqueous K_2CO_3 solution (20 mL). The resulting mixture was extracted with ethyl acetate, and the organic phase was washed with H_2O, dried over Na_2SO_4, and concentrated to provide the crude amino product **7** which was used directly for next step of reaction. All the solid products obtained were dissolved in anhydrous THF solution, followed by the addition of trimethylamine (571 mg, 5.64 mmol). The mixture was cooled to 0°C and then 4-chlorobutyryl chloride (398 mg, 2.82 mmol) or butyryl chloride (300 mg, 2.82 mmol) was added dropwise. After 1 h of stirring at 0 °C, the temperature was raised to room temperature and the stirring was continued for overnight. After removal of the solvent in vacuo, the residue was purified by column chromatography to give **8** (152 mg, yield 66%) as a yellow solid. ^1H NMR (300 MHz, Chloroform-*d*) δ 8.81 (d, *J* = 4.5 Hz, 1H), 8.35 (s, 1H), 8.16 (d, *J* = 16.1 Hz, 1H), 8.07 (s, 1H), 7.66 (dd, *J* = 12.0, 7.4 Hz, 2H), 7.60 – 7.50 (m, 4H), 7.46 (dd, *J* = 10.2, 5.0 Hz, 2H), 7.15 – 7.05 (m, 3H), 4.11 (s, 3H), 3.71 (t, *J* = 6.0 Hz, 2H), 3.63 (s, 3H), 2.70 (t, *J* = 7.0 Hz, 2H), 2.33 – 2.20 (m, 2H); LC-MS: m/z= 429.17 [M+H]$^+$

Synthesis of (E)-4-chloro-N-(4-(4-fluorostyryl)-5,8-dioxo-5,8-dihydroquinolin-6-yl)butanamide (9, SQD1). To a stirred solution of **8** (12 mg, 0.028 mmol) in a mixture of CH_3CN and H_2O (1 mL, 1:1) was added a solution of ceric ammonium nitrate (31 mg, 0.056 mmol) in CH_3CN: H_2O (1 mL, 2:1) dropwise at 0°C. The reaction mixture was stirred at room temperature for 30 min before being diluted with an ice-water slurry (5 mL) and taken up by dichloromethane. The organic layer was combined, dried, concentrated and purified by column chromatography to give **9** (8 mg, yield 81%) as a yellow solid. ^1H NMR (300 MHz, CDCl$_3$) δ 8.94 (s, 1H), 8.43 (s, 1H), 8.24 (d, *J* = 16.1 Hz, 1H), 8.00 (s, 1H), 7.79 (d, *J* = 4.9 Hz, 1H), 7.62 (dd, *J* = 8.2, 5.5 Hz,

2H), 7.27 (d, J = 16.2 Hz, 1H), 7.13 (t, J = 8.5 Hz, 2H), 3.66 (t, J = 6.0 Hz, 2H), 2.71 (t, J = 7.0 Hz, 2H), 2.28 – 2.14 (m, 2H); LC-MS: m/z= 398.90 [M+H]$^+$

Cell culture and reagents. MIA PaCa-2, BxPC-3, PANC-1, KYSE-410, KYSE-70, and T-47D were cultured in RPMI 1640 medium supplemented with 10% FBS (v/v). MDA-MB-468 and MDA-MB-231 were cultured in L-15 medium supplemented with 10% FBS (v/v). HUCCT1 was cultured in RPMI 1640 medium supplemented with 1% penicillin/streptomycin (v/v) and 10% FBS (v/v). TFK1 cells was cultured in RPMI 1640 medium supplemented with penicillin/streptomycin (50 U/mL) and 10% FBS (v/v). Cells were maintained at 37 °C in a humidified atmosphere of 5% CO_2. They were maintained in culture under 40 passages and tested regularly for *mycoplasma* contamination using Plasmo Test (InvivoGen).

Western blotting and antibodies. Cells were lysed in RIPA buffer (25 mM Tris-HCl, pH =7.4, 150 mM NaCl, 1% Nonidet P-40, 0.5% Sodium deoxycholate, 0.1% SDS) supplemented with Halt Protease and Phosphatase Inhibitor Cocktail (Thermo Scientific, 78443). Protein concentration was determined by BCA protein assay kit (Thermo Scientific, 23228, 23224). Unless otherwise described, 25-30 µg of protein was resolved by SDS–polyacrylamide gel electrophoresis (PAGE). Antibodies used for Western blots include C-Jun (Santa Cruz, SC-74543), SESN-2 (Santa Cruz, SC-393195), HK2 (ThermoFisher, 700422), PFKFB4 (ThermoFisher, PA5-15475), HMOX1 (Thermo Fisher, MA1-112), MAP LC3α/β (Santa Cruz, SC-398822), FOSB (Cell Signaling, 2251T), GAPDH (Cell Signaling, 2118S), GABARPAL1 (Cell Signaling, 26632S), PARP (Cell Signaling, 9542S), Cleaved PARP (Cell Signaling, 5625), p-H2AX (Cell Signaling, 9718), MT-CYB (Abcam, ab81215), MT-ATP6 (Abcam, ab192423), MT-ND6 polyclonal antibody (Thermo Fisher, PA5-43532) and tubulin (Santa Cruz, SC-101527).

Author Manuscript

Colony formation assay. Cells were seeded in 24-well tissue culture plates at a density of 500 cells per well or 96-well plates at 250 cells per well. After overnight attachment, cells were treated with compounds for 24 h. NAC or vitamin-E was added 1 h prior to the compound treatments. Then, the media containing compounds was removed and fresh media was added. After 7–10 days, when colonies had fully formed in the DMSO-treated wells, cells were stained with a 0.05% crystal violet solution for 30 min, and then washed with ddH$_2$O to remove excess stain. Plates were imaged using Odyssey Imaging Systems (LI-COR Biosciences) after overnight drying. The colony density was quantified by Licor and ImageJ.

CM-H2DCFDA ROS assay. MIA PaCa-2 cells were seeded in 96-well flat clear-bottom black tissue culture plates at a density of 1.5×10^4 per well. After overnight attachment, the media was removed and 100 µL CM-H$_2$DCFDA dye (10 µM, Thermo Fisher, C6827) in HBSS solution was added to each well at 37 °C for 35–40 min. After removal of the dye solution, cells were washed with pre-warmed DPBS for 2 times and then 80 µL HBSS solution was added. After pretreatment with or without NAC (3 mM), tested compounds were added in HBSS solution at designated concentrations. Fluorescent signal was then measured using CLARIO Star plate reader (Ex: 483 ± 15M; Em: 530 ± 20 nM).

Bru-seq experiment and analysis. MIA PaCa-2 cells were seeded in 10 cm dishes in duplicates. Twenty-four hours later, cells were treated with DMSO, SQD1 (5.4 µM), Mito-Chlor (51 µM), Chlor (233 µM) or H$_2$O$_2$ (50 µM, 150 µM and 300 µM) for 4 h. Bromouridine (Bru) was added to the media during the last 30 min of treatment to a final concentration of 2 mM as previously described (13). Cells were then collected in TRIZOL and total RNA was isolated. The Bru-labeled nascent RNA was immunocaptured using anti-BrdU antibodies conjugated to magnetic beads. The cDNA libraries (Illumina TrueSeq) converted from the bromouridine-labeled RNA were sent for

deep sequencing to the University of Michigan Sequencing Core. Sequencing reads (~40 million per sample) were mapped to the hg38 reference genome. Enriched gene sets were analyzed using GSEA. Hierarchical clustering was performed using $\log_2$FC of gene expression. R programming language (Version 3.5.1) was utilized to produce select figures.

MitoSOX imaging. MIA PaCa-2 cells were seeded in 96-well clear-bottom black tissue culture plates at a density of 5000 cells per well. After overnight attachment, media was removed and 100 μL HBSS solution was added into each well. The cells were treated with SQD1 (5.4 μM), Mito-Chlor (51 μM), chlorambucil (233 μM), TPP (51 μM), antimycin A (15 μM) or DMSO, respectively. After 1-hour incubation at 37˚C, the medium was removed. HBSS working solution with 5 μM MitoSOX dye (Thermo Fisher, M36008) and 4 μg mL^{-1} Hoechst 33342 (Thermo Fisher, H3570) were added and incubated for 15 minutes. Cells were then washed gently three times with warm HBSS buffer before imaging by the OLYMPUS DP80 system with RFP and DAPI filters using the 20 X objective.

DHE staining analyzed by flow cytometry. MIA PaCa-2 cells were seeded in 6-well plates at a density of 400,000 cells per well. After overnight attachment, medium was removed, and the cells were washed with HBSS solution once. A solution of 5 μM DHE dye in HBSS pre-warmed buffer was added to each well. After incubation at 37 °C for 30 min, tested compounds were added. Plates were covered and incubated for an additional hour at 37 °C and protected from light. Staining buffer was carefully aspirated, and 0.5 mL trypsin was added to detach the cells. Complete medium (0.5 mL) was added to each well to neutralize the trypsin and then cells were transferred to centrifugal tubes to pellet the cells. Supernatant was discarded and cells were resuspended in HBSS buffer. The fluorescence of DHE was measured using a flow cytometer (ZE5 cell analyzer, Bio-

Rad) with excitation at 488 nm and emission at 530 nm. At least 10,000 events were collected. Histograms were analyzed by Flowjo (Version 8).

RNA preparation and real-time PCR (RT-PCR). MIA PaCa-2 cells were seeded into 6-well tissue culture plates at a density of 3×10^5 per well and allowed to attach overnight before treating with drugs at specified time. RNAs were collected using Direct-zol RNA Miniprep kit (Zymo Research). RNA (1 μg) from each sample was reverse-transcribed into cDNA using the High-Capacity cDNA Reverse Transcription Kit (Applied Biosystems). RT-PCR was performed using Viia 7 Real-Time PCR System (Thermo Scientific) with TaqMan Gene Expression Master Mix (Thermo Scientific). RT-PCR primers (MT-ND6, MT-ATP6, MT-CYB, HMOX1, GAPDH) were purchased from Thermo Scientific. Relative expression levels were normalized to GAPDH and fold changes in mRNA expression level were evaluated using the $2^{-\Delta\Delta Ct}$ method.

Mitochondrial membrane potential detection. MIA PaCa-2 cells were seeded into 6-well tissue culture plates at a density of 3×10^5 per well and allowed to attach overnight before treating with compounds at specified time. Cells were then resuspended and incubated with 20 nM TMRM (Thermo Fisher, M20036) in HBSS solution at 37 °C for 30 min and protected from light. CCCP (50 μM) was used as a positive control. After removing the dye, the fluorescence intensity was measured by Bio-Rad ZE5 Analyzer flow cytometer (Ex: 561 nm; Em: 590 nm). The percentage of TMRM fluorescence level of the treatment groups compared to the control group represents the relative mitochondrial membrane potential.

Measurement of total cellular ATP in glucose and galactose medium. RPMI 1640 medium (Thermo Fisher, 11875101) was used as glucose medium. Galactose medium was prepared by adding 10 mM galactose (Sigma-Aldrich, G0750) to RPMI 1640 medium with no glucose (Thermo Fisher, 11879020). Cells were seeded into 96-well plates (Corning, 3603) at a density of 10,000

cells/well. The total cellular ATP content was determined 24 hours after compound treatment using the CellTiter-Glo® Luminescence Cell Viability Assay according to the manufacturer's protocol (Promega Corporation, G7570). Luminescence signals were quantified using a scanning microplate reader (BMG Labtech).

Immunoblot. MIA PaCa-2 cells were seeded into 6-well tissue culture plates for 2.5×10^5 cells per well and allowed to attach overnight before treating with appropriate compounds at indicated concentrations. Then, cells were lysed with RIPA buffer in the presence of protease and phosphatase inhibitors. The cells were collected, centrifuged and the pellet was discarded. Protein concentration of whole cell lysate in the supernatant was determined by BCA protein assay kit. Proteins were resolved on 8-15% SDS-PAGE and electrotransferred to transfer membrane (Immobilon®-FL). After incubating in blocking buffer (5% nonfat dry milk in TBST) at room temperature for 1 h, membranes were probed with primary antibody (1:500–1:1000) in blocking buffer overnight at 4 °C. Next day, membranes were washed 3 times for 5 min with TBST, followed by incubation in anti-rabbit or anti-mouse secondary antibody (Dylight 800 4× PEG conjugated; Thermo Scientific; 1:5000) in blocking buffer at room temperature for 1 h. The membranes were washed 3 times with TBST and imaged by Odyssey® CLx Imaging System. Protein levels were quantified by ImageJ 1.52a and the relative density of each band was normalized by respective loading controls.

Statistical analysis. Statistical analysis was conducted using GraphPad Prism (Version 6.0), R programming (Version 3.5.1). All data are shown as mean ± standard deviation from at least 3 independent experiments. Significance levels for assays and immunoblots were determined using the unpaired Student's *t*-test between two groups using Microsoft Excel. Significance levels for transcriptomic profile comparisons were calculated using R.

Acknowledgements

Conflict of Interest

The authors declare no conflict of interest

Authors' Contributions

W. Chen and S.Hu contributed equally to this work. W.C., S.H., M.L., and N.N. wrote and edited the manuscript. Bru-seq experiments were performed by M.P. and S.H.. Bioinformatic analysis was performed by S.H. and M.L.. W.C., S.M., H.L. and X.C. contributed to synthesis of **SQD** compounds. Western blots were performed by W.C., S.H. and H.G.. RT-PCR, TMRM assay was performed by S.H.. DHE staining was done by W.C. Y.X. performed the cellular ATP assay. The project was supervised by N.N..

Keywords: *antitumor, bru-seq, mitochondria transcription, mRNA, reactive oxygen species (ROS)*

Author Manuscript

REFERENCES

[1]   a) D. C. Wallace, *Nat. Rev. Cancer* **2012**, *12*(10), 685-698; b) P. E. Porporato, N. Filigheddu, J. M. B. Pedro, G. Kroemer, L. Galluzzi, *Cell Res.* **2018**, *28*(3), 265-280; c) S. Vyas, E. Zaganjor, M. C. Haigis, *Cell* **2016**, *166*(3), 555-566.

[2]   a) M. G. Vander Heiden, L. C. Cantley, C. B. Thompson, *Science* **2009**, *324*(5930), 1029-1033; b) P. E. Porporato, R. K. Dadhich, S. Dhup, T. Copetti, P. Sonveaux, *Front. Pharmacol.* **2011**, *2*, 49; c) C. E Griguer, C. R Oliva, *Curr. Pharm. Des.* **2011**, *17*(23), 2421-2427.

[3]   C. T. Moraes, S. Srivastava, I. Kirkinezos, J. Oca-Cossio, M. Woischnick, F. Diaz, *Int. Rev. Neurobiol.* **2002**, *53*, 3-23.

[4]   a) D. C. Wallace, *Nat. Rev. Cancer* **2012**, *12*(10), 685; b) P. Desjardins, E. Frost, R. Morais, *Mol. Cell. Biol.* **1985**, *5*(5), 1163-1169; c) P. Desjardins, J.-M. de Muys, R. Morais, *Somat. Cell Mol. Genet.* **1986**, *12*(2), 133-139; d) M. P. King, G. Attardi, *Science* **1989**, *246*(4929), 500-503; e) D. Magda, P. Lecane, J. Prescott, P. Thiemann, X. Ma, P. K. Dranchak, D. M. Toleno, K. Ramaswamy, K. D. Siegmund, J. G. Hacia, *BMC Genomics* **2008**, *9*(1), 521; f) R. Morais, K. Zinkewich-Péotti, M. Parent, H. Wang, F. Babai, M. Zollinger, *Cancer Res.* **1994**, *54*(14), 3889-3896; g) L. R. Cavalli, M. Varella-Garcia, B. C. Liang, *Cell Growth Differ.* **1997**, *8*, 1189-1198; h) F. Weinberg, R. Hamanaka, W. W. Wheaton, S. Weinberg, J. Joseph, M. Lopez, B. Kalyanaraman, G. M. Mutlu, G. S. Budinger, N. S. Chandel, *Proc. Natl. Acad. Sci. U.S.A.* **2010**, *107*(19), 8788-8793.

[5]   E. Benbrik, P. Chariot, S. Bonavaud, M. Ammi-Saïd, E. Frisdal, C. Rey, R. Gherardi, G. Barlovatz-Meimon, *J. Neurol. Sci.* **1997**, *149*(1), 19-25.

Author Manuscript

[6]   E. Segal-Bendirdjian, D. Coulaud, B. P. Roques, J.-B. Le Pecq, *Cancer Res.* **1988**, *48*(17), 4982-4992.

[7]   a) J. T. Madak, N. Neamati, *Curr. Top. Med. Chem.* **2015**, *15*(8), 745-766; b) J. Zielonka, J. Joseph, A. Sikora, M. Hardy, O. Ouari, J. Vasquez-Vivar, G. Cheng, M. Lopez, B. Kalyanaraman, *Chem Rev* **2017**, *117*(15), 10043-10120.

[8]   M. Millard, J. D. Gallagher, B. Z. Olenyuk, N. Neamati, *J. Med. Chem.* **2013**, *56*(22), 9170-9179.

[9]   a) R. A. Tapia, Y. Prieto, G. Zamora, A. Morello, Y. Repetto, *Heterocycl. Commun.* **2000**, *6*(6), 539-544; b) R. Cassis, R. Tapia, J. A. Valderrama, *Synth. Commun.* **1985**, *15*(2), 125-133.

[10]   a) M. T. Paulsen, A. Veloso, J. Prasad, K. Bedi, E. A. Ljungman, B. Magnuson, T. E. Wilson, M. Ljungman, *Methods* **2014**, *67*(1), 45-54; b) S. Hu, Y. Jin, Y. Liu, M. Ljungman, N. Neamati, *Eur. J. Med. Chem.* **2018**, *158*, 884-895.

[11]   C. M. Gustafsson, M. Falkenberg, N. G. Larsson, *Annu. Rev. Biochem.* **2016**, *85*, 133-160.

[12]   N. Sharma, M. S. Pasala, A. Prakash, *Environ Mol. Mutagen.* **2019**, *60*(8), 668-682.

[13]   V. M. Gohil, S. A. Sheth, R. Nilsson, A. P. Wojtovich, J. H. Lee, F. Perocchi, W. Chen, C. B. Clish, C. Ayata, P. S. Brookes, V. K. Mootha, *Nat. Biotechnol.* **2010**, *28*(3), 249-255.

[14]   M. S. Kane, A. Paris, P. Codron, J. Cassereau, V. Procaccio, G. Lenaers, P. Reynier, A. Chevrollier, *Biochem. Pharmacol.* **2018**, *148*, 100-110.

[15]   R. Gozzelino, V. Jeney, M. P. Soares, *Annu. Rev. Pharmacol. Toxicol.* **2010**, *50*, 323-354.

[16]   a) Z. Zhang, L. Zhang, L. Zhou, Y. Lei, Y. Zhang, C. Huang, *Redox biol.* **2019**, *25*, 101047; b) J. D. Malhotra, R. J. Kaufman, *Antioxid. Redox Sign.* **2007**, *9*(12), 2277-2294.

[17]   M. H. Stipanuk, J. E. Dominy Jr, J.-I. Lee, R. M. Coloso, *J. Nutr.* **2006**, *136*(6), 1652S-1659S.

[18]   G. Wu, Y.-Z. Fang, S. Yang, J. R. Lupton, N. D. Turner, *J. Nutr.* **2004**, *134*(3), 489-492.

[19]   F. Z. Chakrama, S. Seguin-Py, J. N. Le Grand, A. Fraichard, R. Delage-Mourroux, G. Despouy, V. Perez, M. Jouvenot, M. Boyer-Guittaut, *Autophagy* **2010**, *6*(4), 495-505.

[20]   a) A. Subramanian, P. Tamayo, V. K. Mootha, S. Mukherjee, B. L. Ebert, M. A. Gillette, A. Paulovich, S. L. Pomeroy, T. R. Golub, E. S. Lander, J. P. Mesirov, *Proc. Natl. Acad. Sci. U.S.A.* **2005**, *102*(43), 15545-15550; b) V. K. Mootha, C. M. Lindgren, K. F. Eriksson, A. Subramanian, S. Sihag, J. Lehar, P. Puigserver, E. Carlsson, M. Ridderstrale, E. Laurila, N. Houstis, M. J. Daly, N. Patterson, J. P. Mesirov, T. R. Golub, P. Tamayo, B. Spiegelman, E. S. Lander, J. N. Hirschhorn, D. Altshuler, L. C. Groop, *Nat. Genet.* **2003**, *34*(3), 267-273.

[21]   S. B. Le, M. K. Hailer, S. Buhrow, Q. Wang, K. Flatten, P. Pediaditakis, K. C. Bible, L. D. Lewis, E. A. Sausville, Y.-P. Pang, *J. Biol. Chem.* **2007**, *282*(12), 8860-8872.

[22]   a) K. Zlotkowski, W. M. Hewitt, P. Yan, H. R. Bokesch, M. L. Peach, M. C. Nicklaus, B. R. O'Keefe, J. B. McMahon, K. R. Gustafson, J. S. Schneekloth, Jr., *Org. Lett.* **2017**, *19*(7), 1726-1729; b) B. Marydasan, B. Madhuri, S. Cherukommu, J. Jose, M. Viji, S. C. Karunakaran, T. K. Chandrashekar, K. S. Rao, C. M. Rao, D. Ramaiah, *J. Med. Chem.* **2018**, *61*(11), 5009-5019.

[23]   a) P. Wardman, *Free Radic. Biol. Med.* **2007**, *43*(7), 995-1022; b) S. K. NaveenKumar, B. N. SharathBabu, M. Hemshekhar, K. Kemparaju, K. S. Girish, G. Mugesh, *ACS Chem. Biol.* **2018**, *13*(8), 1996-2002.

[24]   G. Cheng, M. Zielonka, B. Dranka, S. N. Kumar, C. R. Myers, B. Bennett, A. M. Garces, L. G. Dias Duarte Machado, D. Thiebaut, O. Ouari, M. Hardy, J. Zielonka, B. Kalyanaraman, *J. Biol. Chem.* **2018**, *293*(26), 10363-10380.

[25]   a) T. Vierbuchen, E. Ling, C. J. Cowley, C. H. Couch, X. Wang, D. A. Harmin, C. W. M. Roberts, M. E. Greenberg, *Mol. Cell. Biol.* **2017**, *68*(6), 1067-1082 e1012; b) F. Bejjani, E. Evanno,

K. Zibara, M. Piechaczyk, I. Jariel-Encontre, *Biochim. Biophys. Acta, Rev. Cancer* **2019**, *1872*(1), 11-23.

[26]   A. Loboda, M. Damulewicz, E. Pyza, A. Jozkowicz, J. Dulak, *Cell. Mol. Life Sci.* **2016**, *73*(17), 3221-3247.

[27]   B. Y. Shin, S. H. Jin, I. J. Cho, S. H. Ki, *Free Radic. Biol. Med.* **2012**, *53*(4), 834-841.

[28]   Y. Yang, S. Karakhanova, W. Hartwig, J. G. D'Haese, P. P. Philippov, J. Werner, A. V. Bazhin, *J. Cell. Physiol.* **2016**, *231*(12), 2570-2581.

[29]   a) N. D. Georgakopoulos, G. Wells, M. Campanella, *Nat. Chem. Biol.* **2017**, *13*(2), 136-146; b) S. Pickles, P. Vigie, R. J. Youle, *Curr. Biol.* **2018**, *28*(4), R170-R185.

[30]   a) V. A. Bohr, *Free Radic. Biol. Med.* **2002**, *32*(9), 804-812; b) F. M. Yakes, B. Van Houten, *Proc. Natl. Acad. Sci. U.S.A.* **1997**, *94*(2), 514-519.

[31]   S. D. Cline, *Biochim. Biophys. Acta, Gene Regul. Mech.* **2012**, *1819*(9-10), 979-991.

Graphic figure

The mitochondria targeting nitrogen mustard Mito-Chlor was found to inhibit the transcription of mitochondrial DNA. A search of similar compound lead to the discovery of another mitochondria transcription inhibitor SQD1. The two compounds share a genome-wide similar transcriptomic profile, and both induce mitochondria superoxide and similar cell signaling pathway. This study supports targeting mitochondria as an efficient anticancer therapy.

SQD1
$IC_{50} = 1.3 \pm 0.2 \ \mu M$

Mito-Chlor
$IC_{50} = 42.0 \pm 2.0 \ \mu M$